PHYSICAL REVIEW E **80**, 025202(R) (2009)

Period fissioning and other instabilities of stressed elastic membranes

Benny Davidovitch
Department of Physics, University of Massachusetts, Amherst, Massachusetts 01003, USA
(Received 25 November 2008; revised manuscript received 7 May 2009; published 24 August 2009)

We study the shapes of elastic membranes under the simultaneous exertion of tensile and compressive forces when the translational symmetry along the tension direction is broken. We predict a multitude of morphological phases in various regimes of a two-dimensional parameter space (ϵ, ν) that defines the relevant mechanical and geometrical conditions. These parameters are, respectively, the ratio between compression and tension, and the wavelength contrast along the tension direction. The predicted patterns emerge through new transition and instability mechanisms and include several types of irregular and smooth cascades composed of wrinkles and sharp folds. In particular, the hierarchical morphology predicted under high tension and large wavelength contrast $(\epsilon \ll 1, \nu \gg 1)$, explains recent experimental observations on ultrathin membranes floating on liquid.

DOI: 10.1103/PhysRevE.80.025202 PACS number(s): 46.32.+x, 47.20.Ky, 62.20.D−, 68.60.Bs

Elastic sheets exhibit a remarkable variety of patterns in response to a featureless distribution of forces or geometric constraints. Familiar examples are the crumpled shapes of papers and foils under isotropic confinement [1–3], the periodic arrays of wrinkles on a uniaxially stressed skin [4], and the wavy edge of a plastic sheet that is ripped apart [5]. The realization that essential features of natural [5,6] and man-made [7] films are related to the coupling between geometry and mechanics of thin elastic membranes [1] has inspired a renewed interest in this problem, whose foundations had been set many decades ago [8]. Central questions that guide past and current research in this field are the following: what are the fundamental *instabilities* by which the spatial symmetry of elastic membrane is broken? What are the characteristic features of patterns that emanate from these instabilities? Finally, one may ask—is it possible to classify the rich variety of observed membrane patterns in a "phase diagram," whose axes correspond to a small set of universal *morphologically relevant* parameters?

In this Rapid Communication we address these questions by focusing on a simple system: a homogenous membrane of highly symmetric (rectangular) shape that is bent due to a uniaxial compression (Fig. 1) along $\hat{y}$. We assume that the membrane is under uniform tension (along $\hat{x}$) and that boundary conditions (BCs) at one edge $(x=0)$ forbid the formation of an "ideal" one-dimensional (1D) shape. One may guess that the membrane shape should posses the highest symmetry allowed by the constraints and is thus some superposition of the Fourier modes that compose the ideal bent shape and the deformed edge. A paper sheet that is forced in a similar fashion to Fig. 1 reveals, however, that such highly symmetric shape is rarely obtained. This problem thus enables one to uncover the mechanisms, by which the spatial symmetry associated with the system and imposed constraints, is broken. A tensionless version of this "curtain problem" (with flat edge at $x=0$) was studied by Pomeau and Rica [9], who predicted the emergence of a cascade of sharp folds as $x \to 0$. A central result of our analysis is the prediction of a series of elastic "period fissioning" instabilities that govern the formation of a *smooth* cascade of wrinkles when sufficiently large tension is exerted along $\hat{x}$. This result explains an experimental observation that motivated this Rapid Communication: a repetitive steplike increase in wrinkle periodicity near an edge $(x=0)$ of an ultrathin uniaxially compressed membrane that is floating on liquid [10] and subject to tension and geometric frustration due to strong capillary forces. Furthermore, we identify two dimensionless parameters that represent the mechanical conditions (ϵ is the ratio between compression along $\hat{y}$ and tension along $\hat{x}$) and geometric frustration (ν is the imposed wavelength contrast along $\hat{x}$). Our analysis leads us to conjecture a surprisingly rich phase diagram (Fig. 2) that is spanned by these parameters and describes all possible membrane patterns in this problem. In addition to explaining the observations of [10], we predict the following hierarchical structures: (a) smooth cascades (F_n) with any n generations of wrinkles (for small ϵ and $\nu \lesssim 1/\sqrt{\epsilon}$), (b) irregular shapes (I_n) composed of any k generations of sharp folds (for large ϵ), and (c) mixed patterns $(M_{n,k})$, in which n generations of smooth wrinkles "coexist" with k generations of sharp folds (for small ϵ and $\nu \gtrsim 1/\sqrt{\epsilon}$). This picture raises fundamental questions concerning the nature of morphological phase transitions in elastic membranes that may be related to the emergence of hierarchical patterns in other energy-dominated systems, such as edges of type-I superconductors [11].

We consider a long rectangular membrane (Fig. 1) of thickness $t \ll W, L$, supported on a liquid substrate and bent due to compressive forces along the two edges $y=0, W$, that are relatively displaced by a distance $\Delta \ll W$. If the edges at $x=0, -L$ are free, a 1D sinusoidal wrinkling pattern is formed, whose wavelength $2\pi/q_0$ reflects a balance between the energetic cost of membrane bending and gravity of the lifted liquid mass. A tension along $\hat{x}$ does not affect this ideal 1D pattern. Now we assume that an *unstrained* deformation of the edge $x=0$ imposes there a sinusoidal profile of wave number $q_e=(1+\nu)q_0$ and ask for the energetically favorable membrane configuration under these conditions. This problem is similar to [9], with three crucial differences: (i) we

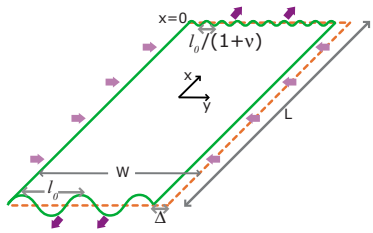

FIG. 1. (Color online) Schematics of membrane geometry.

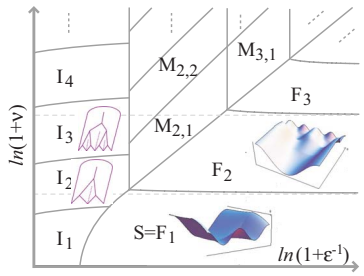

FIG. 2. (Color online) A conjectured phase diagram for stressed membranes ($\tilde{\Delta} \ll 1, \bar{L} \gg 1$). The axis correspond to the parameters (ϵ, ν). The irregular (I_n), period-fissioning (F_n), and mixed $(M_{n,k})$ morphologies are described below.

assume a uniform (x independent) displacement $\Delta \ll W$ (rather than uniform compression $\sigma_{yy}=P$); (ii) we assume a uniform tension $\sigma_{xx}=T$ in $\hat{x}$ (rather than tensionless membrane); and (iii) we assume any positive wavelength contrast $\nu>0$ [rather than a flat edge at $x=0$ that corresponds to $\nu \to \infty$ by Eq. (2a)]. A liquid substrate is assumed both for simplicity and for comparison with the observations of [10]. Our formalism and results are generalizable, however, to wrinkling phenomena in which restoring force is associated with solid substrate or for buckled free-standing membranes. Our analysis proceeds as follows: first, we obtain the energy to quadratic order in $\tilde{\Delta}=\Delta/W$. Second, we show that this approximation is valid only if T is sufficiently large. This leads to conjecture I, concerning a transition (S-I) between smooth patterns (high tension) and irregular ones (low tension). Third, we address the high tension regime and discover the period fissioning instability that leads to the formation of smooth cascade of wrinkles.

To $O(\tilde{\Delta}^2)$, the *areal* energy density of a membrane shape $\zeta(x,y)$ is [10]

$$u = \frac{1}{2}\left(B(\nabla^2 \zeta)^2 + \rho g \zeta^2 + \sigma(x)\left[\left(\frac{\partial \zeta}{\partial y}\right)^2 - 2\tilde{\Delta} \right] + T\left(\frac{\partial \zeta}{\partial x}\right)^2 \right), \quad (1)$$

where the compressive stress $\sigma_{yy}=\sigma(x)$ appears as a Lagrange multiplier that forces *inextensibility* of contour lines parallel to the $\hat{y}$ direction. The membrane bending modulus is $B \sim Et^3$, where E is the Young's modulus [8] and ρ is the liquid density. Let us review first the case when both edges $x=0$ and $-L$ are free [10,12]. Assuming a 1D periodic pattern, $\zeta(x,y)=\zeta \sin(qy)$ one finds

$$\zeta = \frac{2}{q}\sqrt{\tilde{\Delta}}, \quad (2a)$$

$$\frac{u}{\Delta} = -\sigma = \frac{\rho g}{q^2} + Bq^2, \quad (2b)$$

with energy density $u=-\sigma_0 \Delta$ minimized for $q_0=(\rho g/B)^{1/4}$ and $\sigma_0=-2\sqrt{B\rho g}$. The parameter ϵ is hence defined as the ratio $|\sigma_0|/T$. The energy of the shape [Eq. (2)] is $-\sigma_0 \Delta L$, whereas the energy of a *planar* compressed membrane is $\frac{1}{2}Y\tilde{\Delta}^2 WL$, where $Y \sim Et$ is the stretching modulus. The threshold value, below which the membrane remains flat, is thus $\tilde{\Delta}_{min}=2\sigma_0/Y$ ($\tilde{\Delta}_{min} \to 0$ as $t \to 0$). Consider now the case where the edge $x=0$ is forced to take an unstrained sinusoidal shape [Eq. (2a)] with a wave number $q_e=(1+\nu)q_0$. We assume a length L large enough such that away from the deformed edge the membrane recovers its periodic energetically favorable shape with $q=q_0$. A natural guess for the shape is then a state that retains the *highest symmetry* possible under these constraints:

$$\zeta(x,y) = \zeta_0(x)\sin(q_0 y) + \zeta_1(x)\sin(q_1 y), \quad (3)$$

where

$$q_0^2\zeta_0^2 + q_1^2\zeta_1^2 = 4\tilde{\Delta}, \quad (4)$$

and

$$\lim_{x \to X_0} \zeta_1(x) = 0, \quad (5a)$$

$$\lim_{x \to X_1} \zeta_0(x) = 0, \quad (5b)$$

where Eq. (4) is the inextensibility condition (recall that $\tilde{\Delta} \ll 1$) and $X_0=-L$, $X_1=0$, and $q_1=q_e$ are introduced to simplify the forthcoming analysis. As we show below, the simple pattern [Eq. (3)] gives way to distinct types of hierarchical morphologies for most parameters values (ϵ, ν).

The smooth shape [Eq. (3)] favored naturally by the harmonic energy [Eq. (1)] is markedly different from the irregular cascade described by [9] (for $\nu \to \infty$) in the tensionless case $T=0$. This difference reflects the *anharmonic* energy $u_G \sim O(\tilde{\Delta}^4)$ associated with the Gaussian curvature and, hence, strain imposed in the membrane by a wavelength contrast $\nu>0$ [13]. Such energetic cost favors the formation of flat strain-free facets separated by narrow strain-focusing zones [1]. This mechanism underlies the emergence of a sharp folds cascade when $T=0$ [9]. If tension exists, flat facets are penalized by the *harmonic* term $u_T=T(\partial_x \zeta)^2$, and a smooth shape [Eq. (3)] is thus preferable if T is large enough. A transition from irregular to smooth shapes is thus expected if $u_G<u_T$. This inequality implies $\tilde{\Delta} \lesssim T/Y$ [13]. Together with the threshold condition $\tilde{\Delta} \gtrsim |\sigma_0|/Y$, we obtain a necessary condition for the existence of a smooth shape: $\epsilon = |\sigma_0|/T \lesssim 1$. We thus conclude that a transition from an irregular sharply folded pattern [9] to a smooth shape occurs at $\epsilon^{SI} \sim O(1)$. A more detailed analysis shows that ϵ^{SI} increases with ν and that $\epsilon^{SI}(\nu \to 0) > 0$ [14]. Since under tensionless conditions ($\epsilon \to \infty$) with $\nu \to \infty$, the shape is an infinite cascade of folds [9] we conjecture.

Conjecture I. There exists a "branching" series $\{b_n(\epsilon)\}$, such that for (ϵ, ν) with $\epsilon > \epsilon^{SI}(\nu)$, $b_n(\epsilon) < \nu < b_{n+1}(\epsilon)$, the morphology is at phase I_n:n generations of sharp folds.

Conjecture I is depicted in Fig. 2, where the limit $(\epsilon, \nu \to \infty)$ corresponds to Pomeau-Rica infinite cascade.

Hence we focus on the asymptotic regime $[\nu, \epsilon \ll \epsilon^{SI}(\nu)]$, where a smooth shape is expected. Motivated by the hierarchical wrinkling patterns observed in [10], we expect that the highly symmetric pattern [Eq. (3)] undergoes a period fissioning, where it becomes unstable to the emergence of a *discrete set* of alternating Fourier modes with wave numbers $q_1, q_2, \ldots (q_0 < q_i < q_e)$. This inspires us to introduce a type of minimizers, termed as "n strip," to the energy [Eq. (1)] that characterize such broken-symmetry states. These n strips are constructed below from the elementary form (3), hence called "1-strip" [see Figs. 3(b) and 3(c)]. Therefore, we start by analyzing the highly symmetric state [Eq. (3)].

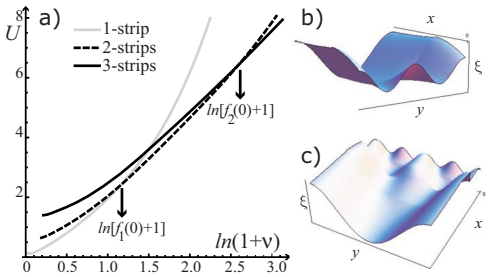

FIG. 3. (Color online) (a) Energies $U_n(\epsilon,\nu)$ of n-strip ($\epsilon \ll 1$ and $n=1-3$) obtained by minimization over all n-strip shapes ($\vec{Q}_n$). Dimensionless convention [Eq. (6)] is used. [(b) and (c)] Computed patterns of 1-strip ($\nu=1$) and 2-strip [$\nu=3$ with $\vec{Q}=(1,2,4)$].

A. 1-strip

We transform to the dimensionless set

$$\bar{x}=\frac{x}{l_T},\quad \bar{y}=\frac{y}{l_T},\quad \bar{\zeta}=\frac{\zeta}{2l_T\sqrt{\epsilon\tilde{\Delta}}},\quad \bar{u}=\frac{u}{4\tilde{\Delta}T\epsilon^2},\quad \bar{\sigma}=\frac{\sigma}{T},\quad a_j=\sqrt{\epsilon}q_j l_T, \tag{6}$$

where $l_T=\sqrt{T/\rho g}$ and $a_0=1$. A minimal energy profile [Eq. (3)] satisfies Euler-Lagrange (EL) equations for the functional (1):

$$M(a_0,\bar{x})\bar{\zeta}_0-(1+2\epsilon a_0^2)\bar{\zeta}_0''+\epsilon^2\bar{\zeta}_0''''=0, \tag{7}$$

$$M(a_1,\bar{x})\bar{\zeta}_1-(1+2\epsilon a_1^2)\bar{\zeta}_1''+\epsilon^2\bar{\zeta}_1''''=0, \tag{8}$$

where

$$a_0^2\bar{\zeta}_0(\bar{x})^2+a_1^2\bar{\zeta}_1(\bar{x})^2=1, \tag{9}$$

and

$$M(a_i,\bar{x})\equiv a_i^4+1+\bar{\sigma}(\bar{x})a_i^2/\epsilon, \tag{10}$$

is the restoring force on 1D wrinkles with wave number $a_i \neq a_0$. With the inextensibility constraint [Eq. (9)], Eqs. (7) and (8) become a nonlinear ordinary differential equation (ODE) for $\bar{\zeta}_0(\bar{x})$ [alternatively, $\bar{\zeta}_1(\bar{x})$]. One may show [14] that for

$$\epsilon \ll 1,\quad a_1 \ll 1/\sqrt{\epsilon}, \tag{11}$$

the fourth derivatives (associated with bending forces due to curvature along $\hat{x}$) are negligible, and the BCs [Eq. (5)] are thus sufficient for solving the resulting second-order ODE. As we show below, the asymptotic behavior at the two ends $\bar{X}_0=-\bar{L}_1$ and $\bar{X}_1=0$, is essential for the iterative construction of n-strip solutions. We therefore address it now. Some algebraic manipulations of Eqs. (5a), (5b), and (7)–(10) [14] yield these asymptotics in terms of two constants C_1, Z_1:

$$\bar{x}\to\bar{X}_0^+:\bar{\zeta}_1=\frac{C_1}{a_1}\sinh[\sqrt{M_+(a_1,a_0,C_1)}(\bar{x}-\bar{X}_0)], \tag{12}$$

$$\bar{x}\to\bar{X}_1^-:\bar{\zeta}_0=\frac{Z_1}{a_0}\sin[\sqrt{-M_-(a_1,a_0,Z_1)}(\bar{x}-\bar{X}_1)], \tag{13}$$

$$M_-\equiv\frac{a_0^4+1-a_0^2\left(a_1^2+\frac{1}{a_1^2}\right)}{1-Z_1^2\left(\frac{a_0}{a_1}\right)^2},\quad M_+\equiv\frac{a_1^4+1-a_1^2\left(a_0^2+\frac{1}{a_0^2}\right)}{1+C_1^2\left(\frac{a_1}{a_0}\right)^2}. \tag{14}$$

It is useful to express the length $\bar{L}_1$ and the constant Z_1, as functions of C_1, which can be obtained using analytic matching or numerical integration [15]. A characteristic highly symmetric solution of the form (3) with $a_1=2$ is presented in Fig. 3(b). The energetic cost $U_1(\epsilon,\nu)$ (where $\nu=a_1-1$) with respect to the 1D periodic wrinkling shape can now be calculated (to leading order in ϵ) using Eq. (1). We found the *linear* behavior: $U_1\approx(\nu-1)$ plotted as a gray solid line (logarithmic scale) in Fig. 3(a).

B. n-strip

Inspired by experimental observations [10] we define n-strip states as follows: n consecutive strips parallel to $\hat{y}$, with series of wave numbers $\vec{Q}_n=(q_0<q_1\cdots<q_{n-1}<q_n=q_e)$ and borderlines $(X_1,\ldots,X_{n-1})$ (with $X_0=-L$ and $X_n=0$). The length of the jth strip is $L_j=X_j-X_{j-1}$ and the profile is described there by a superposition of type (3) with the change in subscripts:

$$0\to j-1,\quad 1\to j. \tag{15}$$

An example of a computed 2-strip is plotted in Fig. 3(c). In order to see how a n-strip solution is constructed *uniquely* from a series of 1-strip solutions, consider some ϵ, a_j [that satisfy Eqs. (11) and (15)], and a 1-strip profile $\bar{\zeta}_{j-1}(\bar{x}),\bar{\zeta}_j(\bar{x})$ in the interval $(\bar{X}_{j-1},\bar{X}_j)$ given by solving Eqs. (5a), (5b), (7)–(10), and (15). The above analysis of 1-strip solutions implies that the length $\bar{L}_j$ and the functions $\bar{\zeta}_{j-1}(\bar{x}),\bar{\zeta}_j(\bar{x})$ are uniquely given by the parameter C_j that appears in the asymptotic [Eqs. (12) and (15)] at $\bar{x}\to\bar{X}_{j-1}^+$. This parameter is determined iteratively by requiring $\bar{\zeta}_{j-1}''(\bar{x}\to\bar{X}_{j-1}^+)=\bar{\zeta}_{j-1}''(\bar{x}\to\bar{X}_{j-1}^-)$, where the last term is determined from the asymptotic [Eq. (13)] of the $(j-1)$th strip in the limit $\bar{x}\to\bar{X}_{j-1}^-$. This "stitching" condition is necessary to avoid a diverging bending force ($\bar{\zeta}_{j-1}''''$) near $\bar{X}_{j-1}$ [16]. Algebraic manipulations similar to those underlying Eqs. (12)–(14) give

$$C_j=\sqrt{\frac{-\left(\frac{a_{j-2}}{a_j}\right)^2M_-(a_{j-1},a_{j-2},Z_{j-1})Z_{j-1}^2}{a_j^4+1-a_j^2\left(a_{j-1}^2+\frac{1}{a_{j-1}^2}\right)+\left(\frac{a_{j-2}}{a_{j-1}}\right)^2M_-(a_{j-1},a_{j-2},Z_{j-1})Z_{j-1}^2}}. \tag{16}$$

The jth strip is thus determined iteratively from the $(j-1)$th strip, and the whole n-strip is fully described by $\vec{Q}_n$.

Next, we used Eq. (1) to compute the energy of n-strips with $n\leq 3$ in the interval $\nu\in(0,20)$. Minimizing energy (for given n and ν) over all series $\vec{Q}_n$ with $q_n=q_0(\nu+1)$, we obtained the result plotted in Fig. 3(a) [17]. This indicates that for $\epsilon\ll 1$, a new symmetry-breaking mechanism exists, where the highly symmetric (1-strip) shape becomes unstable to the formation of n-strips for $\nu>f_1(0)\approx 3.2$. Figure 3 and Eq. (11) lead us to conjecture.

Conjecture II. There exists a period-fissioning series

$\{f_n(\epsilon)\}$, such that for (ϵ,ν) with $\epsilon^{SI}(\nu)<\epsilon<(1+\nu)^2$, $f_n(\epsilon)<\nu<f_{n+1}(\epsilon)$, the morphology is at phase F_n:n-strip shape.

With conjectures I and II, the morphology is described for all (ϵ,ν), except $\epsilon<\epsilon^{SI}(\nu)$, $\nu\gtrsim 1/\sqrt{\epsilon}$. We address this regime, by recalling Eq. (2b), that indicates an increase in the compression $\sigma(x)$ along $\hat{x}$ from σ_0 to $\approx\sigma_0(1+\nu)^2$ at $x=0$. Following our argument underlying conjecture I, we notice that if $\nu^2\gtrsim|\sigma_0|/T=\epsilon$ then $u_T<u_G$ in a region near the edge $x=0$ even for $\epsilon\ll 1$. Hence, for $\nu^2\gtrsim\epsilon$ and $\epsilon<\epsilon^{SI}(\nu)$, we expect a mixed phase $M_{n,k}$: patterns composed of a smooth n-strip away from $x=0$ and k generations of sharp folds near $x=0$.

In the experiments of [10], ultrathin rectangular membranes are under compression $\sigma_0\approx-2\sqrt{\rho g B}$ (since $\tilde{\Delta}\ll 1$) and tension $T\approx\gamma$ along $\hat{x}$, where γ is the water-vapor surface tension. Typical values of B,ρ,γ imply $\epsilon=|\sigma_0|/T<10^{-2}$ [10]. Translational symmetry of wrinkles along $\hat{x}$ is broken by the meniscus (at $x>0$) that is induced by the wrinkled edge $(x=0)$. The meniscus energy $U_{men}(\epsilon,\nu)=\frac{1}{2}\epsilon^{-1}(1+\nu)^{-2}\sqrt{\epsilon^2+(\nu+1)^2}$ [10] favors small amplitude and hence large wave number at $x=0$ [see Eq. (2a)]. A balance with the elastic energy $U_n(\epsilon,\nu)$ of a n-strip [17] gives rise (for $\epsilon\ll 1$) to large wavelength contrast ν beyond threshold for the period fissioning instability. The smooth wrinkling cascades of [10] are thus n-strips. Numerical evaluation of $U_{men}(\epsilon,\nu)+U_n(\epsilon,\nu)$ for various values of n yields minimization of the total energetic cost for $n=2$, in good agreement with the three generations of wrinkles observed in [10]. A detailed comparison between the observed patterns and the theoretically predicted n-strip $(\vec{Q}_n)$ is currently underway [14].

Our model was inspired by experiments [10], in which capillary forces imply both tension and breaking of 1D symmetry (along $\hat{x}$). Our analysis predicts: (i) a series of period fissioning instabilities that give rise to smooth wrinkling cascades under large tension and (ii) the existence of distinct morphological phases of stressed membranes characterized by irregular (I_n), smooth (F_n), and mixed $(M_{n,k})$ patterns. These predictions do not depend on the physical nature of the exerted forces and should be observed under rather general types of forces. Natural questions that await further experimental and computational studies concern the appropriate definition of the parameters ϵ,ν and the possible modifications of Fig. 2 necessary to describe nonideal conditions, such as nonrectangular shape, nonuniform tension, and nonsinusoidal edge. Furthermore, the predicted transition between smooth patterns composed of a finite number of Fourier modes (F_n) and irregular ones (I_n) could be of the analyticity breaking type that is associated with commensurate-incommensurate transitions [18]. This observation and the possible duality hinted by Fig. 2 between transitions among smooth and among irregular patterns may reveal unknown links between patterns of elastic membranes and other energy-minimizing systems, in which hierarchical patterns emerge under boundary forces and geometric constraints [11]. Finally, it is naive to expect that the multitude of patterns associated with inhomogeneous metric [5], biaxial compression [19], or confinement [1–3] are included in a two-dimensional (2D) diagram that characterizes homogenous nearly planar uniaxially compressed membranes. One may ask though, whether Fig. 2 is a cornerstone of a higher-dimensional space spanned by ϵ, ν, and other universal parameters that does describe the rich variety of patterns exhibited by elastic membranes.

The author is grateful to D. Nelson, B. Roman, and P. Chaikin for helpful comments; H. Diamant, I. Dujovne, and J. Machta for critical reading of the Rapid Communication; N. Menon and C. Santangelo for many valuable discussions.

[1] T. A. Witten, Rev. Mod. Phys. **79**, 643 (2007).
[2] M. Ben Amar and Y. Pomeau, Proc. R. Soc. London, Ser. A **453**, 729 (1997).
[3] E. Cerda and L. Mahadevan, Proc. R. Soc. London, Ser. A **461**, 671 (2005).
[4] E. Cerda and L. Mahadevan, Phys. Rev. Lett. **90**, 074302 (2003).
[5] E. Sharon *et al.*, Nature (London) **419**, 579 (2002); B. Audoly and A. Boudaoud, Phys. Rev. Lett. **91**, 086105 (2003).
[6] A. Goriely and M. Ben Amar, Phys. Rev. Lett. **94**, 198103 (2005).
[7] J. Genzer and J. Gorenewold, Soft Matter **2**, 310 (2006).
[8] L. D. Landau and L. M. Lifshitz, *Theory of Elasticity* (Pergamon, New York, 1986).
[9] Y. Pomeau, Philos. Mag. B **78**, 253 (1998); Y. Pomeau and S. Rica, C. R. Acad. Sci., Ser. IIb: Mec., Phys., Chim., Astron. **325**, 181 (1997).
[10] J. Huang *et al.*, http://xxx.lanl.gov/abs/0901.2892
[11] R. Choksi *et al.*, Commun. Pure Appl. Math. **61**, 595 (2008).
[12] L. Pocivavsek *et al.*, Science **320**, 912 (2008).
[13] Assuming for form (3) $\partial_x\zeta_i\sim\zeta_i/l$, with some typical l, we obtain $u_G\sim Yl^{-2}\Sigma_i\zeta_i^4q_i^2$ [1,14] and $u_T\sim Tl^{-2}\Sigma_i\zeta_i^2$. Equation (4) and the inequality $u_G<u_T$ imply $\tilde{\Delta}\lesssim T/Y$.
[14] B. Davidovitch (unpublished).
[15] Analytic method: match the asymptotics [Eqs. (12) and (13)] at some $\bar{X}_0<\bar{x}^*<\bar{X}_1$. Find C_1, Z_1, and $\bar{x}^*$ by solving the three equations expressing continuity of $\bar{\zeta}_0(\bar{x})$ and its first and second derivatives at $\bar{x}^*$ [14]. Numerical method: solve the second-order ODE for $\bar{\zeta}_1(\bar{x})$ with initial conditions $\bar{\zeta}_1(\bar{X}_0)=0$, $\bar{\zeta}_1'(\bar{X}_0)=C_1\sqrt{M_+(a_1,a_0,C_1)}/a_1$, and find $\bar{X}_1$ at which $\bar{\zeta}_1(\bar{X}_1)=1/a_1$ and $\bar{\zeta}_1'(\bar{X}_1)=0$. Notice that for $\bar{L}_1\gg 1$, the asymptotic [Eq. (12)] becomes $\bar{\zeta}_1(\bar{x})\sim e^{(a_1^2-1)(\bar{x}-\bar{L}_1)}$, corresponding to $C_1\sim e^{-\bar{L}_1}\to 0$.
[16] Such divergence implies a highly energetic localized region of large Gaussian curvature, similarly to ridges on crumpled papers [1]. The discontinuity of $\bar{\zeta}_i'$ $(i=j-2,j)$ at $\bar{X}_{j-1}$ leads to putative divergence of *both* tensile $(\bar{\zeta}_i'')$ and bending $(\bar{\zeta}_i'''')$ forces but is cured by a layer of size $\epsilon\ll 1$ whose energetic cost is negligible [14].
[17] We found $U_n(\epsilon,\nu)\sim\alpha_n+\beta_n\log(1+\nu)$, with α_n and $\beta_n>0$ [14].
[18] S. Aubry, in *Solitons in Condensed Matter Physics*, edited by A. Bishp (Springer, New York, 1978).
[19] S. Conti *et al.*, Comput. Methods Appl. Mech. Eng. **94**, 2534 (2004).